



OPEN

# A Gilbert syndrome-associated haplotype protects against fatty liver disease in humanized transgenic mice

Steffen Landerer, Sandra Kalthoff, Stefan Paulusch &amp; Christian P. Strassburg

UDP-glucuronosyltransferases 1A (UGT1A) enzymes are capable of detoxifying a broad range of endo- and xenobiotic compounds, which contributes to antioxidative effects, modulation of inflammation and cytoprotection. In the presence of low-function genetic *UGT1A* variants fibrosis development is increased in various diseases. This study aimed to examine the role of common *UGT1A* polymorphisms in NASH. Therefore, *htgUGT1A*-WT mice and *htgUGT1A*-SNP mice (carrying a common human haplotype present in 10% of the white population) were fed a high-fat Paigen diet for 24 weeks. Serum aminotransferase activities, hepatic triglycerides, fibrosis development and *UGT1A* expression were assessed. Microscopic examination revealed higher hepatic fat deposition and a significant induction of *UGT1A* gene expression in *htgUGT1A*-WT mice. In agreement with these observations, lower serum aminotransferase activities and lower expression levels of fibrosis-related genes were measured in *htgUGT1A*-SNP mice. This was accompanied by reduced PPAR $\alpha$  protein levels in *htgUGT1A*-WT but not in SNP mice. Our data demonstrate a protective effect of a *UGT1A* SNP haplotype, leading to milder hepatic steatosis and NASH. Higher PPAR $\alpha$  protein levels in animals with impaired UGT1A activity are the likely result of reduced glucuronidation of ligands involved in PPAR $\alpha$ -mediated fatty acid oxidation and may lead to the observed protection in *htgUGT1A*-SNP mice.

The growing number of patients with non-alcoholic fatty liver disease (NAFLD) renders this condition one of the most important and common liver disorder worldwide and thus to a significant medical challenge. It is estimated that around 30% of the general American population is affected by NAFLD and more than 85% of these individuals are morbidly obese<sup>1,2</sup>. The prevalence for NAFLD is closely related to obesity and its associated comorbidities and thus leads to an increased mortality rate<sup>3,4</sup>. In view of the high numbers of obese individuals, it is likely that the global incidence of patients with NAFLD will continue to increase. Apart from dietary habits further influences such as gender, age, ethnicity and genetic disorders have been identified as additional risk factors for NAFLD<sup>5</sup>, which has the potential to progress to more severe non-alcoholic steatohepatitis (NASH), cirrhosis and hepatocellular carcinoma (HCC)<sup>6,7</sup>. The molecular events include lobular inflammation, oxidative stress, hepatocellular apoptosis and fibrosis leading to NASH in approximately one quarter of NAFLD individuals<sup>8,9</sup>.

The development of a variety of liver diseases is almost invariably associated with a deregulation of nuclear receptor activation and changes in hepatic enzyme expression patterns. Previous studies have shown that the presence of NAFLD modulates the transcriptional activity of phase I and II enzymes<sup>10,11</sup>. Altered expression levels of hepatic UDP-glucuronosyltransferase *1a* (*Ugt1a*) genes have been detected in (*ob/ob*) mice<sup>12</sup>. Moreover, Hardwick and colleagues identified variations of *UGT1A* expression levels in human liver samples during various stages of NAFLD, but their role in NAFLD progression remain unclear<sup>13</sup>. UGT1A enzymes are localized in the inner membrane of the endoplasmic reticulum and contribute to cytoprotection by catalysing the detoxification of a broad array of endo- and exogenous compounds. These include therapeutic drugs, environmental xenobiotics, reactive metabolites, bilirubin, bile acids, dietary fatty acids and other eicosanoids<sup>14–16</sup>. UGT1A proteins catalyse the covalent conjugation with glucuronic acid rendering lipophilic target substrates water soluble and inactive thereby facilitating biliary or renal elimination<sup>17</sup>. The presence of single nucleotide polymorphisms (SNPs) in the promoter and coding regions modifies the function of *UGT1A* genes<sup>18</sup>. Among more than 100 identified SNPs,

Department of Internal Medicine I, University Hospital Bonn, 53127, Bonn, Germany. e-mail: [christian.strassburg@ukbonn.de](mailto:christian.strassburg@ukbonn.de)

which lead to varying degrees of UGT1A function and expression, the Gilbert syndrome-associated UGT1A1\*28 variant probably represents the best studied *UGT1A* polymorphism<sup>19</sup>. Individuals homozygous for UGT1A1\*28 exhibit a ~70% lower *UGT1A1* promoter activity<sup>20</sup>. Genetic *UGT1A* variants, commonly present in individuals with Gilbert syndrome, have been associated with several liver diseases including HCC and a more severe fibrosis development in patients with hepatitis B and C<sup>21,22</sup>. Based on these findings we designed experiments expecting that enhanced *UGT1A* expression confers a protective effect during hepatic steatosis, NASH development and, as a consequence, in the progression to liver fibrosis. Therefore, the aim of the study was to elucidate the role of *UGT1A* polymorphisms for NASH progression and determine the histopathological consequences for the liver. To this end, humanized transgenic (*htg*) *UGT1A* wild type (WT) and *htgUGT1A*-SNP mice, containing a human haplotype of 10 common occurring *UGT1A* SNPs, were used. Since this SNP haplotype is present in approx. 10% of the white population, our study further allows a risk assessment of NASH progression for a large proportion of the human population. Moreover, special interest was given to the nuclear receptor biology of farnesoid X receptor (FXR) and its downstream target peroxisome proliferator-activated receptor alpha (PPAR $\alpha$ ), which was shown to be downregulated in patients with fatty livers<sup>23</sup>. Both nuclear receptors have been identified as promising therapeutic targets for the treatment of NAFLD due to their ability to control a broad range of hepatic functions involved in lipid and glucose metabolism, inflammation and fibrogenesis<sup>24,25</sup>. Therefore, potential molecular mechanisms leading to the deregulation of FXR and PPAR $\alpha$  activation possibly arising as a consequence of altered UGT1A activity in *htgUGT1A*-SNP mice are discussed and compared to the results of human population studies observed during NAFLD and NASH.

## Results

**Aggravated liver injury and inflammation in *htgUGT1A*-WT mice.** To elucidate the role of UGT1A enzymes in diet-induced liver injury, *htgUGT1A*-WT and SNP mice were fed with a high-fat Paigen diet (HFPD) for 24 weeks and analysed for differences regarding hepatic lipid deposition, triglyceride levels and serum aminotransferase activities. Contrary to our initial hypothesis, the macroscopic examination of the livers revealed higher fat deposition in *htgUGT1A*-WT mice (Fig. 1A). Measurement of hepatic triglycerides (Fig. 1B) confirmed the visual impression and revealed significantly higher triglyceride levels in *htgUGT1A*-WT animals (WT: 77.1  $\mu$ g/mg; SNP: 49.0  $\mu$ g/mg). In comparison to control diet fed animals, both mouse lines showed marked elevations of aspartate aminotransferase (AST) and alanine aminotransferase (ALT) activities after HFPD exposition (Fig. 1C,D). Interestingly, significantly lower AST (24%) and ALT (65%) levels were detected in mice carrying the *UGT1A* SNP variant.

Hepatic steatosis was further analysed by haematoxylin-eosin (H&E) histological staining (Fig. 1E). In agreement with the differential hepatic lipid incorporation, HFPD-treated *htgUGT1A*-WT mice not only showed a higher proportion of steatotic hepatocytes, but also cellular ballooning that was almost exclusively observed in mice carrying the human wild type *UGT1A* gene locus. Moreover, an advanced degree of liver inflammation, indicated by the massive infiltration of inflammatory cells, was observed in *htgUGT1A*-WT mice suggesting the development of NASH (Fig. 1E black arrows). This observation was supported by significant differences in transcriptional activation of the proinflammatory marker genes C-C chemokine ligand 2 (CCL2) and tumour necrosis factor alpha (TNF- $\alpha$ ) (Fig. 1F,G). In *htgUGT1A*-WT mice, a 17.4-fold CCL2 upregulation and a 10.8-fold TNF- $\alpha$  mRNA induction was detected, whereas in the presence of SNPs transcriptional activation of CCL2 (6.4-fold) and TNF- $\alpha$  (2.4-fold) was significantly less evident.

**Attenuated hepatic fibrosis in *htgUGT1A*-SNP mice.** With the intention of determining differences in fibrosis development and hepatic collagen deposition, computational quantification of Sirius red staining and gene expression analysis of profibrotic biomarkers was evaluated. Histological staining showed a higher content of fibrillar collagens, and thus fibrosis development, in *htgUGT1A*-WT mice (Fig. 2A). Computational quantification of Sirius red staining further supported the histological finding and detected 8.4-fold higher percentage portion of red coloured fibrillar collagens in *htgUGT1A*-WT mice (Fig. 2B). Moreover, a 3.0-fold higher transcriptional activation of collagen type 1 alpha 1 (*Col1a1*) in *htgUGT1A*-WT mice supported the results at a molecular level and confirmed the differences in fibrosis development between both mouse lines (Fig. 2C).

Manifestation of liver fibrosis is usually associated with an increased expression of cytokines, chemokines and various key genes influencing fibrogenesis. In *htgUGT1A*-WT mice, HFPD administration caused significantly higher transcriptional activation of the profibrotic markers transforming growth factor beta (TGF- $\beta$ ), connective tissue growth factor (CTGF), platelet-derived growth factor subunit B (PDGFB) and tissue inhibitor metalloprotease 1 (TIMP1), whereas mRNA induction was reduced (TIMP1 and PDGFB) or absent (TGF- $\beta$  and CTGF) in the presence of SNPs (Fig. 2D–G). In combination, these data suggest a protective effect of a common *UGT1A* SNP haplotype during diet-induced steatohepatitis, resulting in attenuated hepatic fibrosis and inflammation.

**Increased *UGT1A* expression in *htgUGT1A*-WT mice.** To further evaluate the potential mechanisms responsible for the observed protective effects in *htgUGT1A*-SNP mice, hepatic *UGT1A* expression was determined in both animal models (Fig. 3A). In the livers of *htgUGT1A*-WT mice, HFPD led to a significant upregulation of mRNA expression of all investigated *UGT1A* genes. In contrast and expectedly, significantly lower transcriptional activation was measured in *htgUGT1A*-SNP mice. Attention was given to the expression of *UGT1A3* representing the only UGT1A isoform capable of glucuronidating bile acids, which in turn are key regulators of nuclear receptors involved in glucose and lipid metabolism<sup>26,27</sup>. In line with the detected mRNA expression results, hepatic UGT1A3 protein quantity was markedly increased in HFPD treated *htgUGT1A*-WT mice (Fig. 3B).

**Reduced expression of FXR and PPAR $\alpha$  in HFPD fed *htgUGT1A*-WT mice.** FXR is known to play a crucial role in mediating effects of bile acids during NAFLD. After diet-induced liver injury, a significant decrease

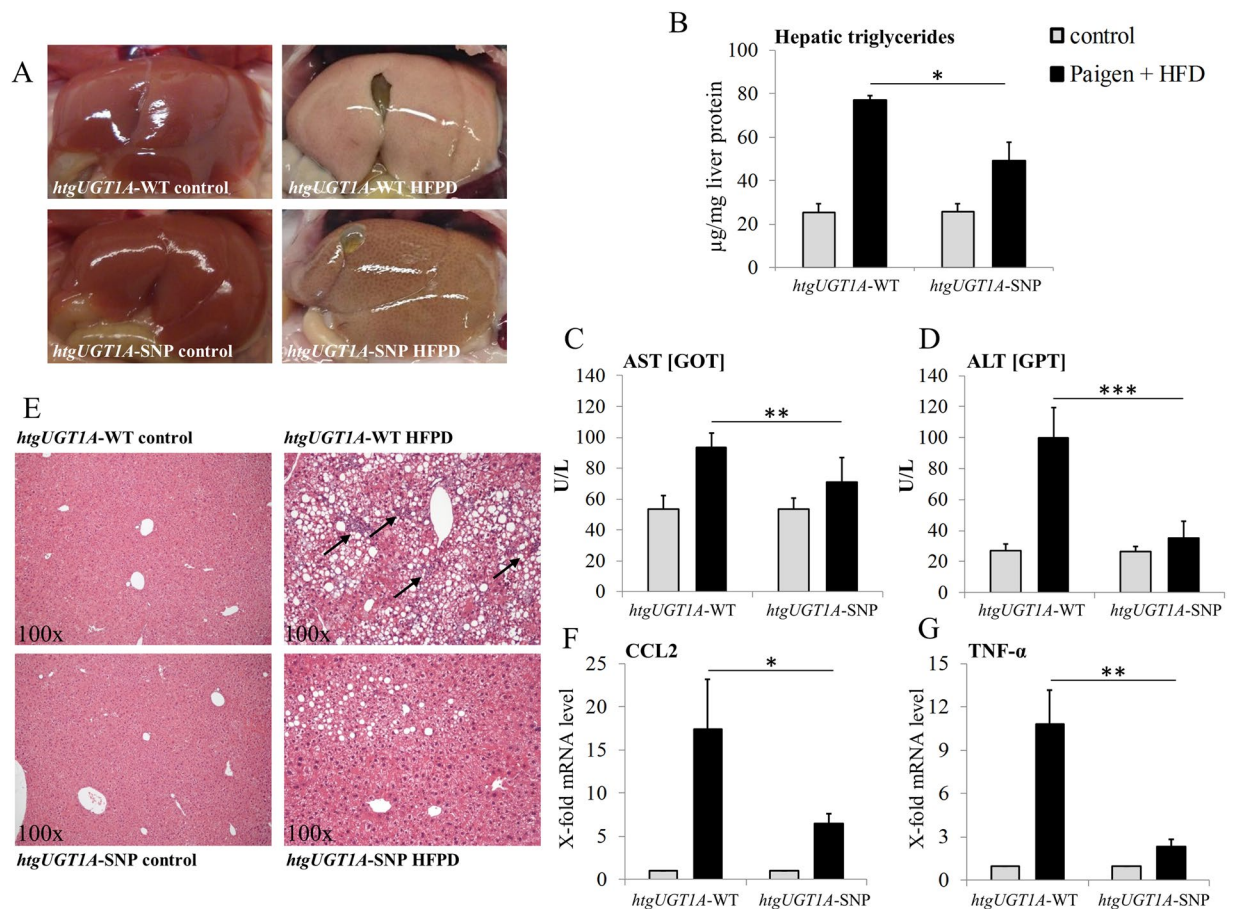


**Figure 1.** Differential effects of 24 weeks high-fat Paigen diet (HFPD) in *htgUGT1A*-WT and SNP mice. **(A)** Macroscopic liver depictions after abdominal opening. Livers of *htgUGT1A*-WT mice fed with HFPD showed a higher degree of steatosis as those of their SNP counterparts. **(B)** Hepatic triglyceride content expressed as µg/mg liver protein. In the presence of SNPs significantly lower levels of triglycerides were detected. **(C)** Representative sections of hematoxylin and eosin (H&E) stained liver tissue (magnification 100×). Hepatocytes of *htgUGT1A*-WT mice showed more fat accumulation and a higher proportion of infiltrated inflammation cells (black arrows). **(D,E)** Liver injury was assessed by serum aspartate aminotransferase (AST) and alanine aminotransferase (ALT) activities. Mice carrying the *UGT1A* SNP haplotype had significantly lower AST and ALT levels. **(F,G)** Gene expression levels of the pro-inflammatory markers C-C chemokine ligand 2 (CCL2) and tumour necrosis factor alpha (TNF-α). Induction of the transcriptional activation was significantly lower in *htgUGT1A*-SNP mice indicating a higher degree of inflammation. Each column represents the mean ± standard deviation. \* $p < 0.05$ ; \*\* $p < 0.01$ ; \*\*\* $p < 0.001$ .

of the FXR mRNA expression was detected in both mouse lines (Fig. 4A). Interestingly, the degree of inhibition reached 58% in *htgUGT1A*-WT mice, compared to only 36% measured in *htgUGT1A*-SNP mice. PPARα is a downstream target of FXR and a well-known mediator of hepatic fatty acid oxidation<sup>28</sup>. The nuclear translocation of PPARα protein was downregulated in HFPD fed *htgUGT1A*-WT mice whereas PPARα activation remained unchanged in *htgUGT1A*-SNP mice (Fig. 4B). These results demonstrate a differential effect of *UGT1A* SNPs for the expression of nuclear receptors involved in cellular protection.

## Discussion

Effects of altered *UGT1A* expression on the pathogenesis of NAFLD and the associated consequences for the pathology of the liver have not been experimentally analysed. Contrary to our expectations and our original hypothesis, the results demonstrate that increased *UGT1A* expression does not protect against NASH progression in a humanized *UGT1A* animal model of NAFLD. The data suggest a protective effect of a common low-function *UGT1A* SNP haplotype in NAFLD/NASH. *HtgUGT1A*-SNP mice exhibited milder hepatic steatosis, significantly lower levels of hepatic triglycerides and a less pronounced elevation of AST and ALT levels compared to *htgUGT1A*-WT mice. Furthermore, a reduced deposition of fibrillar collagens and decreased expression levels of profibrotic and proinflammatory marker genes underscore an attenuated process of liver fibrosis in *htgUGT1A*-SNP mice. This was accompanied by the significant upregulation of *UGT1A* expression levels in *htgUGT1A*-WT mice, compared to a reduced or absent induction in mice carrying the low-function SNP variant.

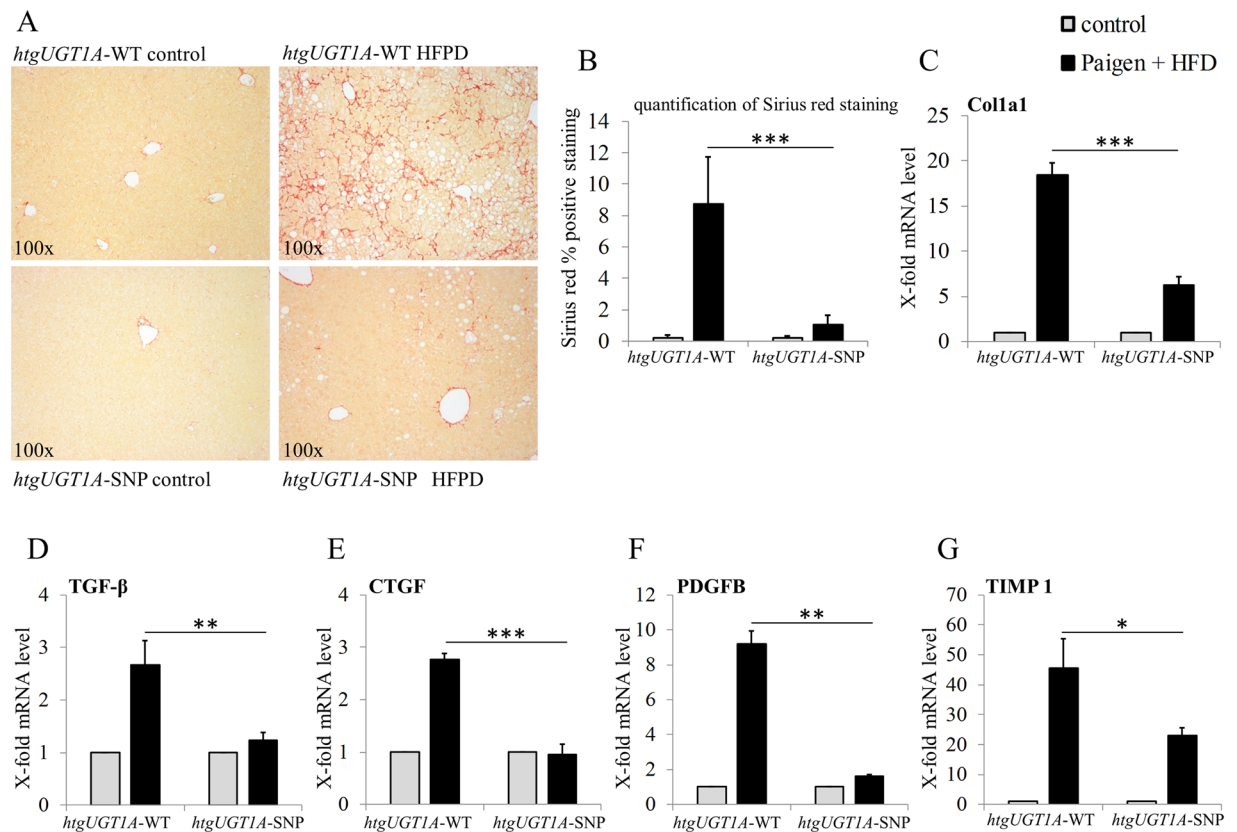


**Figure 2.** Assessment of liver fibrosis in *htgUGT1A*-WT and SNP mice after high-fat Paigen diet (HFPD) treatment. (A) Representative hepatic sections of histological Sirius red staining and (B) computational quantification of Sirius red stained areas. Hepatic collagen deposition was significantly lower in *htgUGT1A*-SNP mice. (C–G) Gene expression levels of the profibrotic biomarkers collagen type 1 alpha 1 (Col1a1), transforming growth factor beta (TGF- $\beta$ ), connective tissue growth factor (CTGF), platelet-derived growth factor subunit B (PDGFB) and tissue inhibitor metalloprotease 1 (TIMP 1) as indicators for severity of liver fibrosis. Transcriptional activation of all depicted fibrosis marker genes was significantly lower in *htgUGT1A*-SNP mice. In case of TGF- $\beta$  and CTGF, minor transcriptional inductions were detected in HFPD-treated *htgUGT1A*-SNP mice. Graphs are expressed as means  $\pm$  standard deviation. \* $p < 0.05$ ; \*\* $p < 0.01$ ; \*\*\* $p < 0.001$ .

To date, contradictory results have been published in various cohort-studies investigating an association between genetic *UGT1A* variants and human NAFLD. In line with our study, a decreased risk of paediatric NAFLD has been reported in 234 obese Taiwanese children associated with a low-activity *UGT1A1* gene variant<sup>29</sup>. Similarly, a case-control study with 641 adult patients suspected to have NAFLD reported an inverse association between unconjugated hyperbilirubinemia and the histopathological severity of liver damage in NASH<sup>30</sup>. In contrast, genome-wide association studies and other genetic studies of human NAFLD have failed to find an association between *UGT1A1* polymorphisms and NAFLD<sup>31</sup>. A likely explanation for the inconsistent data reported in these studies may involve the presence of *UGT1A* polymorphisms found in other isoforms than *UGT1A1*. Since many SNPs exist in linkage-disequilibrium with each other, the inter-individual *UGT1A* sequence variation is highly variable<sup>22</sup>. Previously, we were able to show that 76% of homozygous *UGT1A1*\*28 carriers, a genotype that is associated with elevated bilirubin levels, were simultaneously homozygous for 9 other *UGT1A* polymorphisms<sup>32</sup>. Therefore, a combination of multiple polymorphisms in distinct *UGT1A* isoforms is suggested to be responsible for the observed hepatoprotective effects in this study and maybe also for the differential results in human population studies only considering polymorphisms in the *UGT1A1* gene.

A molecular mechanism potentially triggering the *UGT1A* SNP-associated protective effects could include the impaired glucuronidation of molecules that function as ligands for nuclear receptors (i.e. FXR or PPAR $\alpha$ ) involved in lipid homeostasis. A specific example is the *UGT1A*-mediated glucuronidation of dietary fatty acids, such as arachidonic acids and its metabolites 20-hydroxyeicosatetraenoic acid (20-HETE) and leukotriene B4 (LTB4), which have been previously identified as potent PPAR $\alpha$  activators<sup>33</sup> and as *UGT1A3* or *UGT1A9* substrates<sup>14,34,35</sup>. In this context, Little *et al.* suggested that *UGT1A* enzymes may function as modulators for the availability of fatty acids to act as ligands for nuclear receptors. Therefore, the decreased *UGT1A* expression in many different isoforms, as present in *htgUGT1A*-SNP mice, may lead to higher intracellular levels of ligands involved in a broad array of lipid homeostasis signalling pathways. The impaired capacity of *htgUGT1A*-SNP mice to eliminate potential FXR or PPAR $\alpha$  ligands may improve the PPAR $\alpha$ -mediated mitochondrial fatty acid oxidation, hepatic fatty acid uptake, peroxisomal beta-oxidation or other crucial processes of lipid metabolism and

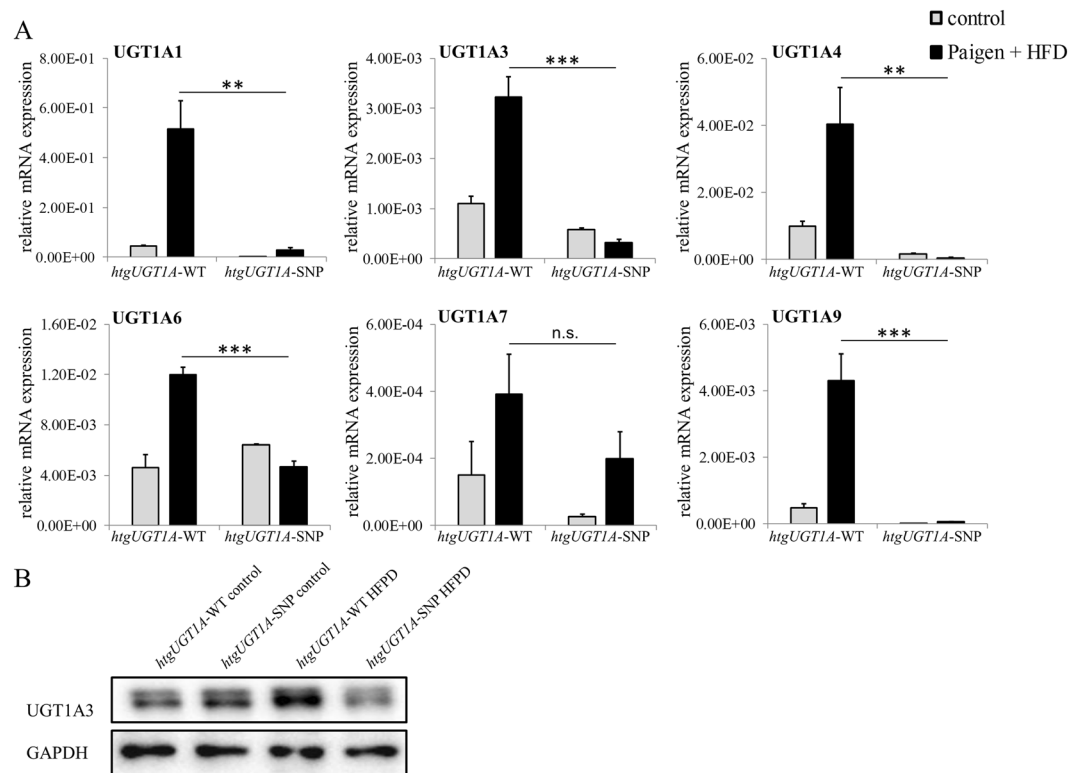


**Figure 3.** Hepatic *UGT1A* regulation in *htgUGT1A-WT* and SNP mice after high-fat Paigen diet (HFPD) treatment. **(A)** Hepatic mRNA expression levels of *UGT1A* isoforms relative to mouse  $\beta$ -actin. In *htgUGT1A-WT* mice, HFPD treatment led to a significant transcriptional upregulation of all depicted *UGT1A* isoforms, whereas in the presence of SNPs *UGT1A* induction was reduced (*UGT1A1* and *UGT1A9*) or absent and remained below those observed in WT carriers. **(B)** Western blot analysis of hepatic *UGT1A3* protein quantity. Higher protein amount was detected in *htgUGT1A-WT* mice. Graphs are expressed as means  $\pm$  standard deviation. n.s. not significant; \* $p < 0.05$ ; \*\* $p < 0.01$ ; \*\*\* $p < 0.001$ .

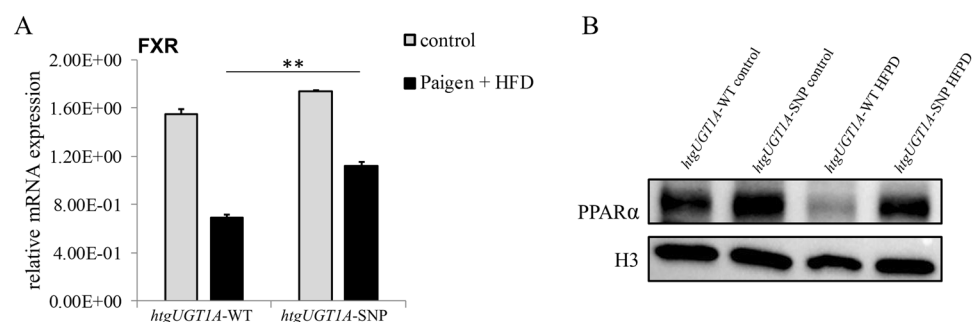


**Figure 4.** Hepatic mRNA expression and nuclear protein quantity of nuclear receptors in *htgUGT1A-WT* and SNP mice after high-fat Paigen diet (HFPD) treatment. **(A)** Enhanced inhibition of farnesoid X receptor (FXR) mRNA expression level was detected in *htgUGT1A-WT* mice (58%) compared to *htgUGT1A-SNP* mice (36%). **(B)** Western blot analysis of nuclear peroxisome proliferator-activated receptor alpha (PPAR $\alpha$ ) protein levels. Significantly reduced PPAR $\alpha$  protein amount was measured in HFPD-treated *htgUGT1A-WT*, in contrast to unchanged levels in the presence of SNPs. Graphs are expressed as means  $\pm$  standard deviation. \* $p < 0.05$ ; \*\* $p < 0.01$ ; \*\*\* $p < 0.001$ .

leads to the lower degree of hepatic steatosis. Moreover, polymorphisms in the specific *UGT1A3* isoform, which is the major enzyme in the *UGT1A* gene locus capable to catalyse the glucuronidation of bile acids, are likely to also contribute to the beneficial effects and mediated independently of the *UGT1A1*\*28 promoter polymorphism. Bile acid levels were shown to be elevated in patients with NASH<sup>36</sup> and have been identified as FXR inducers<sup>37</sup>. Due to higher *UGT1A3* expression in *htgUGT1A-WT* animals potentially leading to increased glucuronidation of FXR-inducing bile acids, unaffected *UGT1A3* activity is suggested to reduce FXR activation leading to an impaired FXR-induced PPAR $\alpha$ -mediated fatty acid oxidation. Reduced FXR expression as well as lower levels of

nuclear PPAR $\alpha$  protein in *htgUGT1A*-WT mice underline this hypothesis and lead to the conclusion that the differential regulation of both nuclear receptors is likely to be directly linked to the differential expression of *UGT1A* genes. Although glucuronidation of bile acids has previously been demonstrated in mice<sup>38</sup>, it is important to note that bile acid glucuronidation only constitutes a relevant detoxification pathway in humans. In mice, however, it is predominantly converted into muricholic acid and only minute amounts are present<sup>39,40</sup>. Even though the relative occurrence of this conjugation reaction is minor in mice, the proposed physiological role is likely to occur in humans. In addition, the FXR downstream targets small heterodimer partner and PPAR $\alpha$  have previously been shown to initiate the downregulation of the lipogenic master regulator sterol regulatory element-binding protein 1c (SREBP-1c)<sup>28,41</sup>. Therefore, increased FXR expression in *htgUGT1A*-SNP mice might be associated with reduced SREBP-1c activation and consequently with a downregulation of *de novo* lipogenesis.

As a consequence, the combination of two or more polymorphisms in different *UGT1A* isoforms may be a more accurate indicator for the occurrence of *UGT1A* SNP-associated liver protection during NAFLD or NASH in human population studies. Along with PPAR $\alpha$  and FXR, other nuclear receptors such as constitutive androstane receptor, pregnane X receptor, liver X receptor and hepatocyte nuclear factor 4 have also been implicated in the pathogenesis of NAFLD<sup>24</sup> while also being involved in the transcriptional regulation of *UGT1A* genes<sup>42</sup>. Therefore, polymorphisms in *UGT1A* genes may ultimately lead to various metabolic changes in patients with NAFLD and large-scale OMICS analysis might be necessary to get a full picture of the transcriptomic and proteomic alterations associated with this common *UGT1A*-SNP genotype. However, we cannot fully exclude that the observed effects are influenced by the murine *Ugt1a* enzymes which are also expressed in *htgUGT1A*-WT and SNP mice. This leads to an increased glucuronidation capacity in both mouse lines, which is lower in *htgUGT1A*-SNP mice. Therefore, further studies with *Ugt1a* knockout mice simultaneously carrying the human *UGT1A*-WT or *UGT1A*-SNP transgene would be needed to exclude the effects of non-physiologically high levels of glucuronidation.

In conclusion, our data indicate a protective effect of a Gilbert syndrome-associated *UGT1A* haplotype leading to milder hepatic steatosis during the development of NASH. Higher expression of *UGT1A* enzymes was observed in *htgUGT1A*-WT mice, while *htgUGT1A*-SNP mice showed lower serum aminotransferase levels and reduced hepatic collagen deposition. Due to the decreased PPAR $\alpha$  protein and lower FXR expression levels in *htgUGT1A*-WT mice, we hypothesize that increased *UGT1A* expression may lead to the facilitated elimination of potential ligands involved in lipid homeostasis.

## Methods

**Animal model and experimental design.** For animal experiments, previously described 8–10 week-old *htgUGT1A*-WT and SNP mice were used<sup>32,43</sup>. As both mouse lines contain the human *UGT1A* transgene in addition to the murine *Ugt1a* gene locus, the glucuronidation capacity of both animal models is likely above the physiological levels in non-transgenic C57Bl/6 mice, which is, due to the presence of 10 common *UGT1A* polymorphisms, significantly lower in *htgUGT1A*-SNP mice. Male mice of each genotype were divided into two groups consisting of six to eight animals. Both groups were either fed a regular chow or a HFPD for 24 weeks. The HFPD was purchased from the Altromin GmbH & Co. KG Company (Seelenkamp, Germany) and contained a raw fat content of 42% in which fat contributes 70% of total energy requirements. This diet is further characterized by the addition of 1.25% cholesterol and 0.5% sodium cholate. All mice had *ad libitum* access to water and chow and were kept at 22 °C with a 12 hour day/night cycle in the Central Animal Facility of the University Hospital Bonn. 10 days before HFPD administration *htgUGT1A* mice received a 4% raw fat containing diet to adapt animals to the change of dietary components. All experiments were performed and in accordance to the “German Animal-Protection Law” and the relevant guidelines of the Local Institutional Animal Care unit of our university (Haus für experimentelle Therapie, Bonn, Germany) and approved by the relevant North Rhine-Westphalian state-agency for Nature, Environment and Consumer Protection (LANUV, Germany) under the file reference LANUV 84-02.04.2016.A483.

**Tissue collection and biochemical analysis.** After HFPD treatment, animals were sacrificed for organ and blood collection. For biochemical analysis of serum ALT and AST activities, the collected blood was centrifuged at 4.800 rpm for 10 min to remove blood cells. The supernatant was stored at –20 °C until analysis by means of a Fuji DRI-CHEM NX500i serum analyser.

Organ samples were immediately snap-frozen in liquid nitrogen and stored at –80 °C until use. The right lateral lobe was separated before, fixed in 4% paraformaldehyde for three days, subsequently embedded in paraffin and then used for pathohistological examinations.

**Histological staining and computational analysis.** Paraffin-embedded liver sections were trimmed into 2  $\mu$ m thick slices, and stained in 0.1% Sirius red solution (DirectRed 80 in saturated picric acid) for detection of fibrous collagen tissue. The Sirius red positive stained area was quantified using ImageJ software (U.S. National Institutes of Health; <http://rsb.info.nih.gov/ij/>) and shown as percentage positive staining of the total section area. Images were analysed from four randomly selected images (magnification 100 $\times$ ) of each animal and were averaged. H&E staining was applied to visualize lipid-droplets within hepatocytes, cellular ballooning and infiltration of inflammatory cells according to a standard protocol procedure with minor modifications<sup>44</sup>.

**Triglyceride measurement.** Hepatic triglyceride levels were photometrically determined using the Triglyceride Colorimetric Assay Kit (Cayman Chemicals). 300 mg snap-frozen liver tissue was hydrolysed according to manufacturer’s instructions and analysed in duplicates using a MultiSkan GO microplate reader at 540 nm.

**Gene expression analysis.** RNA isolation from snap-frozen liver samples, cDNA synthesis and gene expression analysis by qPCR were performed as described previously<sup>45</sup>. The assays listed below were purchased

from Thermo Scientific and used for quantification of inflammatory and fibrosis-related gene expression levels. These include C-C chemokine ligand 2 (CCL2; Mm00441442\_m1), tumour necrosis factor alpha (TNF- $\alpha$ ; Mm00443260\_g1), collagen type 1 alpha 1 (Col1a1; Mm00801666\_g1), transforming growth factor beta (TGF- $\beta$ ; Mm01178820\_m1), platelet-derived growth factor subunit B (PDGFB; Mm00440677\_m1) connective tissue growth factor (CTGF; Mm01192933\_g1) and tissue inhibitor metalloprotease 1 (TIMP1; Mm01341361\_m1). Expression levels were normalized relative to mouse beta-actin and expressed as fold mRNA levels compared to untreated *htgUGT1A*-WT or SNP mice.

**Western blot analysis.** 60 mg of frozen liver tissue was homogenized in RIPA extraction buffer containing protease inhibitor cocktail and subsequently incubated for 1 h on a shaking plate at 4 °C. After centrifugation (13,000 rpm, 10 min, 4 °C), the supernatant was used for Western blot analysis. Nuclear extraction tissue specimens were prepared using Nuclear Extraction Kit (Abcam) according to manufacturer's instructions. For SDS-PAGE separation, 30  $\mu$ g of protein was boiled at 95 °C for 5 min in Laemmli sample buffer, separated on a 10% acrylamide gel and blotted onto a nitrocellulose membrane *via* electrotransfer using the Trans-Blot<sup>®</sup>-Turbo transfer system. Incubation with primary antibodies (anti UGT1A3, Abnova H00054659-M02, anti GAPDH, Santa Cruz sc-32233, anti PPAR $\alpha$ , Santa Cruz sc-398394 and anti H3 Abcam (ab12079)) was carried out in 5% dry milk. Appropriate secondary antibodies (Santa Cruz, sc-516102 and sc-2054) were used and protein was visualized by chemoluminescence with the use of ChemiDOC MP imaging system (Supplementary Figure S1,S2).

**Statistical analysis.** Data are expressed as mean  $\pm$  SD determined by one-way analysis of variance followed by Students *t*-test to define significance. A pool of six to eight mice in each HFPD group was analysed (four mice per control group); *p* values below 0.05 were considered as statistically significant.

Received: 27 January 2020; Accepted: 30 April 2020;

Published online: 26 May 2020

## References

- McCullough, A. J. Epidemiology of the metabolic syndrome in the USA. *J. Dig. Dis.* **12**, 333–40, <https://doi.org/10.1111/j.1751-2980.2010.00469.x> (2011).
- Younossi, Z. M. *et al.* Global epidemiology of nonalcoholic fatty liver disease—Meta-analytic assessment of prevalence, incidence, and outcomes. *Hepatology* **64**, 73–84, <https://doi.org/10.1002/hep.28431> (2016).
- Vernon, G., Baranova, A. & Younossi, Z. M. Systematic review: the epidemiology and natural history of non-alcoholic fatty liver disease and non-alcoholic steatohepatitis in adults. *Aliment. Pharmacol. Ther.* **34**, 274–85, <https://doi.org/10.1111/j.1365-2036.2011.04724.x> (2011).
- Flegal, K. M., Carroll, M. D., Kit, B. K. & Ogden, C. L. Prevalence of obesity and trends in the distribution of body mass index among US adults, 1999–2010. *Jama* **307**, 491–7, <https://doi.org/10.1001/jama.2012.39> (2012).
- Perumpail, B. J. *et al.* Clinical epidemiology and disease burden of nonalcoholic fatty liver disease. *World J. Gastroenterol.* **23**, 8263–8276, <https://doi.org/10.3748/wjg.v23.i47.8263> (2017).
- Tiniakos, D. G., Vos, M. B. & Brunt, E. M. Nonalcoholic fatty liver disease: pathology and pathogenesis. *Annu. Rev. Pathol.* **5**, 145–71, <https://doi.org/10.1146/annurev-pathol-121808-102132> (2010).
- Sanyal, A. J. NASH: A global health problem. *Hepatol. Res.* **41**, 670–4, <https://doi.org/10.1111/j.1872-034x.2011.00824.x> (2011).
- Marra, F., Gastaldelli, A., Svegliati Baroni, G., Tell, G. & Tiribelli, C. Molecular basis and mechanisms of progression of non-alcoholic steatohepatitis. *Trends Mol. Med.* **14**, 72–81, <https://doi.org/10.1016/j.molmed.2007.12.003> (2008).
- Kleiner, D. E. & Makhlof, H. R. Histology of Nonalcoholic Fatty Liver Disease and Nonalcoholic Steatohepatitis in Adults and Children. *Clin. Liver Dis.* **20**, 293–312, <https://doi.org/10.1016/j.cld.2015.10.011> (2016).
- Fisher, C. D. *et al.* Hepatic cytochrome P450 enzyme alterations in humans with progressive stages of nonalcoholic fatty liver disease. *Drug. Metab. Dispos.* **37**, 2087–94, <https://doi.org/10.1124/dmd.109.027466> (2009).
- Hardwick, R. N., Fisher, C. D., Canet, M. J., Lake, A. D. & Cherrington, N. J. Diversity in antioxidant response enzymes in progressive stages of human nonalcoholic fatty liver disease. *Drug. Metab. Dispos.* **38**, 2293–301, <https://doi.org/10.1124/dmd.110.035006> (2010).
- Xu, J., Kulkarni, S. R., Li, L. & Slitt, A. L. UDP-glucuronosyltransferase expression in mouse liver is increased in obesity- and fasting-induced steatosis. *Drug. Metab. Dispos.* **40**, 259–66, <https://doi.org/10.1124/dmd.111.039925> (2012).
- Hardwick, R. N. *et al.* Altered UDP-glucuronosyltransferase and sulfotransferase expression and function during progressive stages of human nonalcoholic fatty liver disease. *Drug. Metab. Dispos.* **41**, 554–61, <https://doi.org/10.1124/dmd.112.048439> (2013).
- Little, J. M., Williams, L., Xu, J. & Radominska-Pandya, A. Glucuronidation of the dietary fatty acids, phytanic acid and docosahexaenoic acid, by human UDP-glucuronosyltransferases. *Drug. Metab. Dispos.* **30**, 531–3, <https://doi.org/10.1124/dmd.30.5.531> (2002).
- Strassburg, C. P. Pharmacogenetics of Gilbert's syndrome. *Pharmacogenomics* **9**, 703–15, <https://doi.org/10.2217/14622416.9.6.703> (2008).
- Bock, K. W. Functions and transcriptional regulation of adult human hepatic UDP-glucuronosyl-transferases (UGTs): mechanisms responsible for interindividual variation of UGT levels. *Biochem. Pharmacol.* **80**, 771–7, <https://doi.org/10.1016/j.bcp.2010.04.034> (2010).
- Strassburg, C. P. & Kalthoff, S. UDP-Glucuronosyltransferases in Metabolism of Drugs and Other Xenobiotics. Wiley-VCH, 67–116, <https://doi.org/10.1002/9783527630905.ch3> (2012).
- Strassburg, C. P., Nguyen, N., Manns, M. P. & Tukey, R. H. Polymorphic expression of the UDP-glucuronosyltransferase UGT1A gene locus in human gastric epithelium. *Mol. Pharmacol.* **54**, 647–54 (1998).
- Strassburg, C. P., Kalthoff, S. & Ehmer, U. Variability and function of family 1 uridine-5'-diphosphate glucuronosyltransferases (UGT1A). *Crit. Rev. Clin. Lab. Sci.* **45**, 485–530, <https://doi.org/10.1080/10408360802374624> (2008).
- Bosma, P. J. *et al.* The genetic basis of the reduced expression of bilirubin UDP-glucuronosyltransferase 1 in Gilbert's syndrome. *N. Engl. J. Med.* **333**, 1171–5, <https://doi.org/10.1056/nejm199511023331802> (1995).
- Tang, K. S., Lee, C. M., Teng, H. C., Huang, M. J. & Huang, C. S. UDP-glucuronosyltransferase 1A7 polymorphisms are associated with liver cirrhosis. *Biochem. Biophys. Res. Commun.* **366**, 643–8, <https://doi.org/10.1016/j.bbrc.2007.11.125> (2008).
- Strassburg, C. P. Gilbert-Meulengracht's syndrome and pharmacogenetics: is jaundice just the tip of the iceberg? *Drug. Metab. Rev.* **42**, 168–81, <https://doi.org/10.3109/03602530903209429> (2010).
- Francque, S. *et al.* PPARalpha gene expression correlates with severity and histological treatment response in patients with non-alcoholic steatohepatitis. *J. Hepatol.* **63**, 164–73, <https://doi.org/10.1016/j.jhep.2015.02.019> (2015).

24. Trauner, M. & Halilbasic, E. Nuclear receptors as new perspective for the management of liver diseases. *Gastroenterology* **140**(1120–1125), e1–12, <https://doi.org/10.1053/j.gastro.2011.02.044> (2011).
25. Han, C. Y. Update on FXR Biology: Promising Therapeutic Target? *Int J Mol Sci* **19**, <https://doi.org/10.3390/ijms19072069> (2018).
26. Erichsen, T. J. *et al.* Regulation of the human bile acid UDP-glucuronosyltransferase 1A3 by the farnesoid X receptor and bile acids. *J. Hepatol.* **52**, 570–8, <https://doi.org/10.1016/j.jhep.2010.01.010> (2010).
27. Halilbasic, E., Claudel, T. & Trauner, M. Bile acid transporters and regulatory nuclear receptors in the liver and beyond. *J. Hepatol.* **58**, 155–68, <https://doi.org/10.1016/j.jhep.2012.08.002> (2013).
28. Pineda Torra, I. *et al.* Bile acids induce the expression of the human peroxisome proliferator-activated receptor alpha gene via activation of the farnesoid X receptor. *Mol. Endocrinol.* **17**, 259–72, <https://doi.org/10.1210/me.2002-0120> (2003).
29. Lin, Y. C., Chang, P. F., Hu, F. C., Chang, M. H. & Ni, Y. H. Variants in the UGT1A1 gene and the risk of pediatric nonalcoholic fatty liver disease. *Pediatrics* **124**, e1221–7, <https://doi.org/10.1542/peds.2008-3087> (2009).
30. Hjelkrem, M., Morales, A., Williams, C. D. & Harrison, S. A. Unconjugated hyperbilirubinemia is inversely associated with non-alcoholic steatohepatitis (NASH). *Aliment. Pharmacol. Ther.* **35**, 1416–23, <https://doi.org/10.1111/j.1365-2036.2012.05114.x> (2012).
31. DiStefano, J. K. *et al.* Genome-wide analysis of hepatic lipid content in extreme obesity. *Acta Diabetol.* **52**, 373–82, <https://doi.org/10.1007/s00592-014-0654-3> (2015).
32. Ehmer, U. *et al.* Gilbert syndrome redefined: a complex genetic haplotype influences the regulation of glucuronidation. *Hepatology* **55**, 1912–21, <https://doi.org/10.1002/hep.25561> (2012).
33. Boek, K. W. Roles of human UDP-glucuronosyltransferases in clearance and homeostasis of endogenous substrates, and functional implications. *Biochem. Pharmacol.* **96**, 77–82, <https://doi.org/10.1016/j.bcp.2015.04.020> (2015).
34. Bushee, J. L., Liang, G., Dunne, C. E., Harriman, S. P. & Argikar, U. A. Identification of saturated and unsaturated fatty acids released during microsomal incubations. *Xenobiotica* **44**, 687–95, <https://doi.org/10.3109/00498254.2014.884253> (2014).
35. Jarrar, Y. B. *et al.* Determination of major UDP-glucuronosyltransferase enzymes and their genotypes responsible for 20-HETE glucuronidation. *J. Lipid Res.* **55**, 2334–42, <https://doi.org/10.1194/jlr.m051169> (2014).
36. Aranha, M. M. *et al.* Bile acid levels are increased in the liver of patients with steatohepatitis. *Eur. J. Gastroenterol. Hepatol.* **20**, 519–25, <https://doi.org/10.1097/meg.0b013e3282f4710a> (2008).
37. Lew, J. L. *et al.* The farnesoid X receptor controls gene expression in a ligand- and promoter-selective fashion. *J. Biol. Chem.* **279**, 8856–61, <https://doi.org/10.1074/jbc.m306422200> (2004).
38. Zhou, X. *et al.* PPARalpha-UGT axis activation represses intestinal FXR-FGF15 feedback signalling and exacerbates experimental colitis. *Nat. Commun.* **5**, 4573, <https://doi.org/10.1038/ncomms5573> (2014).
39. Alnouti, Y., Csanaky, I. L. & Klaassen, C. D. Quantitative-profiling of bile acids and their conjugates in mouse liver, bile, plasma, and urine using LC-MS/MS. *J. Chromatogr. B Anal. Technol. Biomed. Life Sci.* **873**, 209–17, <https://doi.org/10.1016/j.jchromb.2008.08.018> (2008).
40. Takahashi, S. *et al.* Cyp2c70 is responsible for the species difference in bile acid metabolism between mice and humans. *J. Lipid Res.* **57**, 2130–2137, <https://doi.org/10.1194/jlr.m071183> (2016).
41. Fuchs, C. D., Claudel, T., Scharnagl, H., Stojakovic, T. & Trauner, M. FXR controls CHOP expression in steatohepatitis. *FEBS Lett.* **591**, 3360–3368, <https://doi.org/10.1002/1873-3468.12845> (2017).
42. Hu, D. G., Meech, R., McKinnon, R. A. & Mackenzie, P. I. Transcriptional regulation of human UDP-glucuronosyltransferase genes. *Drug. Metab. Rev.* **46**, 421–58, <https://doi.org/10.3109/03602532.2014.973037> (2014).
43. Kalthoff, S., Landerer, S., Reich, J. & Strassburg, C. P. Protective effects of coffee against oxidative stress induced by the tobacco carcinogen benzo[alpha]pyrene. *Free. Radic. Biol. Med.* **108**, 66–76, <https://doi.org/10.1016/j.freeradbiomed.2017.03.006> (2017).
44. Itagaki, H., Shimizu, K., Morikawa, S., Ogawa, K. & Ezaki, T. Morphological and functional characterization of non-alcoholic fatty liver disease induced by a methionine-choline-deficient diet in C57BL/6 mice. *Int. J. Clin. Exp. Pathol.* **6**, 2683–96 (2013).

## Acknowledgements

The study was supported by grants from the Deutsche Forschungsgemeinschaft project STR 493/8-1 (C.P.S.).

## Author contributions

S.L. performed experiments, analyses and interpretation of data and drafted the manuscript. S.K. contributed to analyses, drafted the manuscript and supervised the study. S.P. performed experiments and contributed to data analyses. C.P.S. performed administrative support, contributed to data interpretation and analysis, obtained funding, supervised and designed the study and revised the manuscript.

## Competing interests

The authors declare no competing interests.

## Additional information

**Supplementary information** is available for this paper at <https://doi.org/10.1038/s41598-020-65481-4>.

**Correspondence** and requests for materials should be addressed to C.P.S.

**Reprints and permissions information** is available at [www.nature.com/reprints](http://www.nature.com/reprints).

**Publisher's note** Springer Nature remains neutral with regard to jurisdictional claims in published maps and institutional affiliations.



**Open Access** This article is licensed under a Creative Commons Attribution 4.0 International License, which permits use, sharing, adaptation, distribution and reproduction in any medium or format, as long as you give appropriate credit to the original author(s) and the source, provide a link to the Creative Commons license, and indicate if changes were made. The images or other third party material in this article are included in the article's Creative Commons license, unless indicated otherwise in a credit line to the material. If material is not included in the article's Creative Commons license and your intended use is not permitted by statutory regulation or exceeds the permitted use, you will need to obtain permission directly from the copyright holder. To view a copy of this license, visit <http://creativecommons.org/licenses/by/4.0/>.

© The Author(s) 2020